Inverse Finite Element Characterization of Soft Tissues

M. Kauer[1], V. Vuskovic[2], J. Dual[1], G. Szekely[3], and M. Bajka[4]

[1] Centre of Mechanics, ETH Zurich, 8092 Zurich, Switzerland
martin.kauer@imes.mavt.ethz.ch
[2] Institute of Robotics, ETH Zurich, 8092 Zurich, Switzerland
[3] Computer Vision Group, ETH Zurich, 8092 Zurich, Switzerland
[4] Department of Gynaecology, University Hospital, 8091 Zurich, Switzerland

Abstract. In this work a tissue aspiration method for the *in-vivo* determination of biological soft tissue material parameters is presented. An explicit axisymmetric finite element simulation of the aspiration experiment is used together with a Levenberg-Marquardt algorithm to estimate the material model parameters in an inverse parameter determination process. Soft biological tissue is modelled as a viscoelastic, non-linear, nearly incompressible, isotropic continuum. Viscoelasticity is accounted for by a quasi-linear formulation. The aspiration method is validated experimentally with a synthetic material. *In-vivo* (intra-operatively during surgical interventions) and *ex-vivo* experiments were performed on human uteri.

1 Introduction

Precise biomechanical characterization of soft tissues has recently attracted much attention in medical image analysis and visualization. Tissue elasticity can deliver valuable diagnostic information. Procedures as palpation have been used for centuries in medical diagnosis. On the other hand, current computer-assisted systems for medical diagnosis, therapy and training are increasingly relying on the availability of procedures allowing a realistic quantitative prediction of the mechanical behaviour of soft tissues.

Surgical navigation, as stereotaxy for limited access brain surgery [1] or image guided orthopaedic navigation [2] often relies on pre-operative images, which have to be aligned with the actual anatomy of the patient during operation. While efficient and precise algorithms have been developed for rigid registration [3], these can only be applied if organ deformation between the radiological data acquisition and the intervention can be excluded. Several studies underline the importance of duly considering elastic tissue deformation in neurosurgery [4] or even in orthopaedic applications [5].

Another area, where soft tissue modelling plays an important role is the development of virtual reality based simulators for surgery training. In addition to several academic research projects in the field of laparoscopic [6,7,8], arthroscopic

W. Niessen and M. Viergever (Eds.): MICCAI 2001, LNCS 2208, pp. 128–136, 2001.

[9] or eye surgery [10] simulators, e.g., a large number of commercial products is already available on the market.

The performance of the simulation in both application areas critically depends on the availability of appropriate methods for calculating soft tissue deformation. Besides highly simplified physically inspired models for laparoscopic training [6,7,11] or interpolative algorithms for landmark-based non-rigid matching [12], several attempts have been published to apply methods based on continuum mechanics. Finite element based simulation of soft tissue deformation has been applied both in surgical simulators [13,14] and elastic image registration especially in neurosurgical applications [15].

While the applied methods sometimes even allow fully volumetric modelling with non-linear effects [14], even the most sophisticated simulation algorithms are of limited use without precise information about the elastic properties of living tissue. Unfortunately, only very limited quantitative data are available about the biomechanical properties of soft tissues, especially for the *in-vivo* characterization of human organs. This is primarily due to the extreme technical and ethical demands on such experiments. In many cases direct access to the internal organs is necessary, which cannot be achieved during the usual surgical procedures without significantly disturbing or prolonging the intervention.

Most traditional methods of material testing like tensile experiments or compression techniques cannot be performed under such circumstances. Indentation methods have been used successfully for *in-vivo* experiments both on the skin [16] and on internal organs during surgery [17]. The resulting tissue deformation is sometimes measured by imaging techniques like ultrasound [18] or MR [19]. Surgical instruments have also been equipped with force-sensing capabilities allowing elasticity measurements [17,20]. These techniques have, however, disturbing drawbacks: they are restricted to one-dimensional testing, they lack well-defined boundary conditions during the experiment and often fail to address the viscoelastic properties of the tissue. MR elastography, allowing to spatially map and quantify small displacements caused by propagating harmonic mechanical waves [21] opened the way for volumetric non-invasive imaging of elastic properties in non-homogeneous organs. The resulting very small displacements (usually 1 mm or less) and the frequency range used do not allow, however, to predict the tissue behaviour in the range of the strains and strain rates observed during surgical interventions.

With the tissue aspiration method presented here we address the following targets: we generate well defined mechanical boundary conditions during the experiment, we are able to induce relatively large tissue deformations (depending on the maximum aspiration pressure) and the time dependent resolution of the deformation allows us to describe the viscoelastic properties of the tissue at a time scale relevant for actual surgical procedures.

2 Methods

2.1 Aspiration Experiment

In this work the experimental data used to characterize the soft tissues is acquired with a tissue aspiration experiment. The tissue aspiration instrument used is shown in Fig. 1. It was developed at the Institute of Robotics at the ETH Zurich. In the tissue aspiration experiment the aspiration tube is put against the target tissue and a weak vacuum is generated in the tube by connecting the aspiration tube to a low-pressure reservoir. A small mirror, placed next to the aspiration hole at the bottom of the tube, reflects the side-view of the aspirated tissue towards the video camera placed on top of the instrument. An optic fibre connected to a light source illuminates the tissue surface. The video camera grabs the images of the aspirated tissue with a frequency of approximately 25 Hz. The aspiration pressure is measured simultaneously with a pressure sensor. Only the profile of the aspirated tissue, represented by the outermost contour of the surface, is used to characterize the deformation. We assume that the experiment

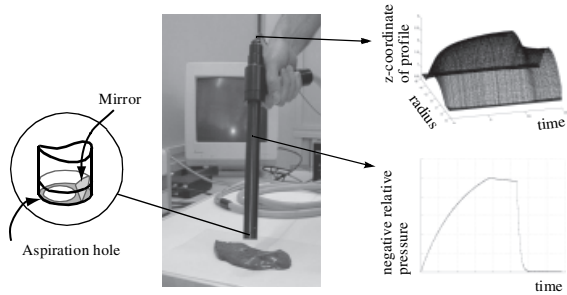

Fig. 1. Tissue Aspiration Experiment

occurs under axisymmetric conditions. Since tissues are in general anisotropic, the condition of axisymmetry will never be met exactly in the experiments.The resulting pressure and profile histories are the two data sets used to evaluate the aspiration experiments. With the profile data of the undeformed tissue a finite element model of the tissue surface is generated. The pressure data is applied to the surface of the finite element model as a surface load in order to simulate the aspiration experiment.

2.2 Soft Tissue Models

The soft tissue material models constitute a very important part of the simulation of the aspiration experiment. Due to their high water content soft biological tissues can be approximated as nearly incompressible materials. The

following form of the strain energy function depending on the reduced invariants $J_1,\ J_2,\ J_3$ of the right Cauchy-Green deformation tensor $\mathbf{C}$ was used in an explicit displacement-pressure finite element formulation [21]

$$\bar{W} = \sum_{i=1}^{N} \mu_i (J_1 - 3)^i + \frac{1}{2}\kappa (J_3 - 1)^2. \tag{1}$$

The μ_i [N/m^2] are material parameters and κ [N/m^2] is the bulk modulus of the material. The degree of non-linearity of this constitutive equation can be determined with the parameter N. By setting $N = 1$ a nearly incompressible neo-Hookean material formulation results. The synthetic material employed in the experimental validation of the aspiration method and the human uteri are modelled with the strain energy function according to Eq. (1).

The viscoelastic material properties are modelled with a quasi-linear approach. The second Piola-Kirchhoff stresses $\mathbf{S}(t + \Delta t)$ at time $t + \Delta t$ in the material are additively composed of a purely elastic part $\mathbf{S}^e$ and a part incorporating the history dependence of the stresses

$$\mathbf{S}(t + \Delta t) = \mathbf{S}^e(\mathbf{C}(\mathbf{x}, t + \Delta t)) + \int_0^{t+\Delta t} \sum_{i=0}^{N_d} (c_i e^{-(t+\Delta t-s)/\tau_i} \frac{\partial}{\partial s} \mathbf{S}^e_{dev}(\mathbf{C}(\mathbf{x}, s)))ds \tag{2}$$

$$\mathbf{S}^e_{dev} = 2\partial(\sum_{i=1}^{N} \mu_i (J_1 - 3)^i / \partial \mathbf{C}), \qquad \mathbf{S}^e = 2\partial \bar{W}(J_1, J_2, J_3)/\partial \mathbf{C}. \tag{3}$$

The spectrum of $N_d + 1$ relaxation times τ_i with corresponding weighting factors c_i in Eq. (2) is used to model the viscoelastic material properties. Depending on the degree N of the strain energy function from Eq. (1) and on the number N_d+1 of relaxation times used in the spectrum approximation of Eq. (2) the following material constants are determined by fitting the simulation of the aspiration experiment to the real aspiration experiment: $\mu_i, i = 1 \ldots N$ and $c_i, i = 1 \ldots N_d$. These parameters are grouped in the parameter vector $\mathbf{p}$. The bulk modulus κ of the material and the different relaxation times τ_i are not included in the parameter determination but set constant.

2.3 Inverse Finite Element Parameter Estimation

The employed material law represents the basis of the inverse parameter estimation. The material law is chosen according to *a priori* knowledge of the mechanical properties of the target tissue. The determination of the parameters contained in the chosen material law is then done by comparing the experimental and the simulated tissue profiles (Fig. 2). The quality of the match of the simulated data and the experimental data is measured by the objective function $o(\mathbf{p})$, which consists of the squared differences between simulated and experimentally determined profile data. The optimization algorithm searches for an optimal set of material parameters in order to minimize the objective function

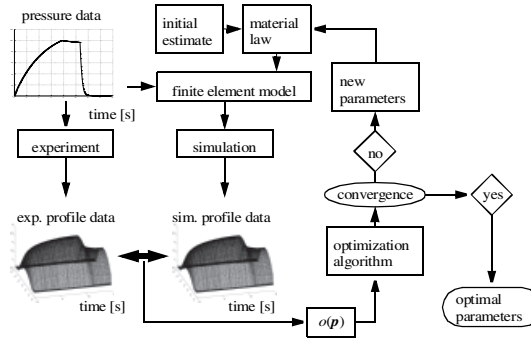

Fig. 2. Flow chart for parameter estimation algorithm

$o(\mathbf{p})$. The parameters corresponding to the computed minimum of the objective function are assumed to represent the real tissue parameters. From the many available algorithms for the optimization of the parameter vector $\mathbf{p}$ we chose the Levenberg-Marquardt method, which has already been shown to work well in finite strain applications [22],[23].

3 Results

3.1 Experimental Validation of the Method

An experimental validation of the aspiration method was performed on a synthetic material by predicting the behaviour in a tensile test with parameters obtained from the aspiration tests. Silgel, a very soft gel-like material, proved to be an ideal material to test the aspiration method. In tensile tests the neo-Hookean material formulation showed to adequately model the silgel material. The following four relaxations times are used to model the viscoelastic properties relevant for the stretch rates in the aspiration and the tensile experiments $\tau_0 = 0.036$ [s], $\tau_1 = 0.36$ [s], $\tau_2 = 3.6$ [s], $\tau_3 = 36$ [s]. The largest relaxation time $\tau_3 = 36$ [s] was determined by optimization from an aspiration experiment. The other relaxation times were equally distributed to obtain a good spectrum approximation. The values obtained for the different material model parameters from the aspiration experiment were then used to simulate tensile experiments. In Fig. 3 the force-elongation curves predicted by these simulations are compared to the corresponding experimentally determined force-elongation curves for different stretch rates. A good agreement between the predicted and the measured data is observed. A good material characterization with the aspiration technique was also possible by using only estimated values for the relaxation times τ_i.

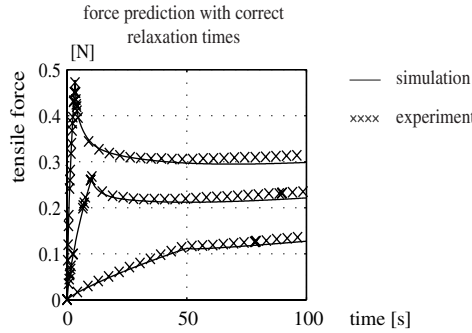

Fig. 3. Comparison of predicted force-elongation curves and experimentally determined data

3.2 In-Vivo Measurements on Human Uterus

The tissue aspiration technique was for the first time applied *in-vivo* on human tissue. In collaboration with the Department of Gynaecology of the University Hospital in Zurich intra-operative measurements on the human uterus were performed. From the continuum-mechanical point of view the uterus represents a very complex tissue. The uterus is a complex multilayered structure with strongly anisotropic properties. On the other hand it is of great advantage for us that the *hysterectomy* (removal of the uterus) is a quite frequently performed surgical intervention and we therefore have the chance to perform measurements on the organ before and after it is excerpted. In some of the cases the excerpted uteri show pathological changes. Three aspiration experiments are performed at different positions before the uterus is removed, then three measurements at the same locations on the removed uterus. The three positions are a ventral and a dorsal position and a position close to the fundus of the uterus. Due to the short duration of 20 seconds of the aspiration experiments the obtained material data is only valid for simulations within this time frame. Since we do not have any data regarding the viscoelastic relaxation times of the human uterus we use the following spectrum of relaxation times for our quasi-linear viscoelastic model $\tau_0 = 0.1$ [s], $\tau_1 = 1.0$ [s], $\tau_2 = 10.0$ [s]. The observed, strongly viscoelastic properties of the uterus would certainly require the inclusion of larger relaxation times in the material model but a robust determination of their weighting factors c_i calls for experiments of long duration which are not possible under *in-vivo* conditions. Tensile experiments performed by Yamada [24] on uteri of rabbits indicate a nearly linear stress-elongation behaviour of the uteri in tensile experiments up to extension ratios of 40%. We therefore assume that the human uterus mechanically behaves similar and use the following strain energy function to model the human uterus

$$\bar{W} = \mu_1(J_1 - 3) + \mu_2(J_1 - 3)^2 + \frac{1}{2}\kappa(J_3 - 1)^2. \tag{4}$$

Fig. 4. Intra-operative experiment on human uterus during a hysterectomy

κ is set to $\kappa = 10^7$ [N/m^2]. Up to now *in-vivo* and *ex-vivo* measurements on six uteri were performed. These six measurements led to five data sets which

	location of performed aspiration experiment	μ_1 [Pa]	μ_2 [Pa]	c_0 []	c_1 []	c_2 []
uterus 3 in-vivo	ventral	1239	829	1.4	7.1	4.7
	dorsal	3044	1879	2.9	3.3	1.6
	fundus	3477	3580	0.5	5.0	1.8
uterus 3 ex-vivo	ventral	894	1306	1.7	3.4	1.9
	dorsal	708	3525	16.0	0.1	0.8
	fundus	754	2914	16.8	1.5	1.6

Table 1. Parameters for the polynomial material law obtained from the in-vivo and ex-vivo aspiration experiments performed on uterus 3

could be evaluated with the inverse parameter estimation algorithm, one data set showed too large a noise component. Stress-stretch curves simulated with the parameters gained from the aspiration experiments are shown in Fig. 5, the corresponding material parameters estimated for uterus 3 are given in Table 1. The time involved for one measurement is approximately one day where all the time needed for the preparatory work, e.g. for getting the patients' consent and having the aspiration instrument sterilized, is not counted here.

4 Discussion

The presented soft tissue aspiration method allows to determine the parameters of mechanical models for soft tissues under *in-vivo* conditions. An experimental validation of the aspiration method with a synthetic material showed that very good predictions of the material behaviour can be made also for states of deformation different from the one in the aspiration experiment. For the first time the aspiration method was employed intra-operatively under *in-vivo* conditions

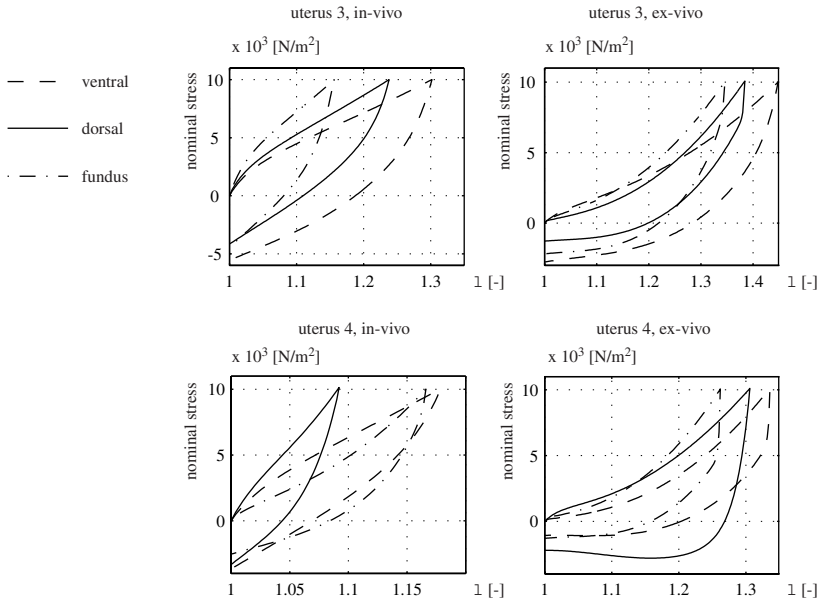

Fig. 5. Stress-stretch curves predicted with data from aspiration experiments on uterus 3 and uterus 4 at a stretch rate of ± 0.02 [1/s]

on human uteri. A pronounced decrease in the uterine tissue stiffness was visible between the *in-vivo* and the *ex-vivo* measurements. The intersample variation of the tissue stiffness of all measurements seemed to be slightly higher than the stiffness variation observed on the single uteri. The maximum differences in stiffness observed in all performed measurements on the uteri were approximately equal in the *in-vivo* and the *ex-vivo* measurements. A statistical interpretation of the mechanical properties of the uterus does not seem appropriate due to the relatively small number of experiments performed.

References

1. H.F. Reinhardt: CT-guided real-time stereotaxy, Acta Neurochir. Suppl. (Wien) 46, pp. 107-8, 1989
2. A.M. Di Gioia, B. Jaramaz (Eds.): Medical Robotics and Computer-Assisted Orthopaedic Surgery, Operative Techniques in Orthopaedics 10(1), 2000
3. J.B.A. Mainz, M.A. Viergever: A survey of medical image registration, Med. Image Analysis 2(1) pp. 1-36, 1998
4. D.L.G. Hill, C.R. Maurer, R.J. Maciunas, J. A. Barwise, J.M. Fitzpatrick, M.Y. Wang: Measurement of Intraoperative Brain Surface Deformation under a Craniotomy, Neurosurgery, 43(2) pp. 514-526, 1998
5. J.A. Little, D.L.G. Hill, D.J. Hawkes: Deformations Incorporating Rigid Structures, Comp. Vision Image Underst. 66(2), pp. 223-232, 1997

6. U. Kuenapfel, H. Krumm, C. Kuhn, M. Huebner, B. Neisius: Endosurgery simulation with kismet, a flexible tool for surgical instrument design, operation room planning and VR technology based abdominal surgery training, B. Groettrup (Ed.), Proc. Virtual Reality World95, pp. 165-171, 1995
7. C. Baur, D. Guzzoni, O. Georg: Virgy, A virtual reality and force feedback based endoscopy surgery simulator, Proc. MMVR98, pp. 110-116, 1998
8. G. Szekely, et.al.: Virtual Reality-Based Simulation of Endoscopic Surgery, Presence 9(3), pp. 310-333, 2000
9. R. Ziegler, W. Mueller, G. Fischer, M. Goebel: A virtual reality medical training system, Proc. CVRMed95, pp. 282-286, 1995
10. M. Schill, C. Wagner, M. Hennen, H-J. Bender, R. Maenner: Eyesi - a simulator for intra-ocular surgery, Proc. 2nd MICCAI Conf, pp. 1166-1174, 1999
11. S. Gibson: 3d chainmail, a fast algorithm for deforming volumetric objects, Proc. Symp. Interactive Comp. Graphics, pp. 149-154, 1997
12. M. Fornefett, K. Rohr, H.S. Stiehl: Elastic Registration of Medical Images Using Radial Basis Functions with Compact Support, Proc. CVPR99, pp. 402-407, 1999
13. S. Cotin, H. Delingette, N. Ayache: Real-Time Volumetric Deformable Models for Surgery Simulation using Finite Elements and Condensation, Proc. Eurographics96, pp. 57-66, 1996
14. G. Szekely, Ch. Brechbuehler, R. Hutter, A. Rhomberg, N. Ironmonger, P. Schmid: Modeling of soft tissue deformation for laparoscopic surgery simulation, Medical Image Anal. 4, pp. 57-66, 2000
15. S.K. Kyriacou, D. Davatzikos: A Biomechanical Model of Soft Tissue Deformation with Applications to Non-rigid Registration of Brain Images with Tumor Pathology, Proc. MICCAI98, pp. 531-538, 1998
16. A.P. Pathak, M.B. Silver-Thorn, C.A. Thierfelder, T.E. Prieto: A rate-controlled indentor for in vivo analysis of residual limb tissues, IEEE Trans. Rehab. Eng. 6(1), pp. 12-20, 1998
17. F.J. Carter, T.G. Frank, P.J. Davies, D. McLean, A. Cuschieri: Biomechanical Testing of Intra-abdominal Soft Tissues, Med. Image Analysis, in press
18. J. Ophir, I. Cespedes, P. Ponnekanti, Y. Yazdi, X. Li: Elastography, a quantitative method for imaging the elasticity of biological tissues, Ultrasonic Imaging 13, pp. 111-134, 1991
19. J.B. Fowlkes et.al.: Magnetic resonance imaging techniques for detection of elasticity variation, Med. Phys 22(11), Pt. 1, pp. 1771-1778, 1995
20. R. Muthupillai, D.J. Lomas, P.J. Rossman, J.F.Greenleaf, A. Manduca, R.L. Ehman: Magnetic Resonance Elastography by Direct Visualization of Propagating Acoustic Strain Waves, Science 269, 99. 1854-1857, 1995
21. T. Sussman, K.J. Bathe: A Finite Element Formulation for Nonlinear Incompressible Elastic and Inelastic Analysis, Journal Computers & Structures, Vol. 26, pp. 357-409, 1987
22. S. K. Kyriacou, C. Schwab, J. D. Humphrey: Finite Element Analysis of Nonlinear Orthotropic Hyperelastic Membranes, Computational Mechanics, Vol. 18, pp. 269-278, 1996
23. M. J. Moulton, L. L. Creswell, R. L. Actis, K. W. Myers, M. W. Vannier, B. A. Szab, M. K. Pasque, An Inverse Approach to Determining Myocardial Material Properties, Journal of Biomechanics, Vol. 28, pp. 935-948, 1995
24. H. Yamada, Strength of Biological Materials, The William & Wilkins Company, Baltimore, 1970